Available online at www.sciencedirect.com
SCIENCE DIRECT®
Atmospheric Environment 39 (2005) 5013–5024
ATMOSPHERIC ENVIRONMENT
www.elsevier.com/locate/atmosenv

Driving forces for ammonia fluxes over mixed forest subjected to high deposition loads

J. Neirynck[a,*], A.S. Kowalski[b], A. Carrara[c], R. Ceulemans[d]

[a]*Institute for Forestry and Game Management, Gaverstraat 4, B-9500, Geraardsbergen, Belgium*
[b]*Departamento de Física Aplicida, Facultad de Ciencias, Universidad de Granada, Calle Fuentenueva, SP-18071, Granada, Spain*
[c]*Fundacion CEAM, Parque Technologico, Calle Charles H. Darwin 14, SP-46980, Paterna (Valencia), Spain*
[d]*Department of Biology, University of Antwerp, Universiteitsplein 1, B-2610, Wilrijk (Antwerp), Belgium*

Received 29 September 2004; received in revised form 5 April 2005; accepted 11 May 2005

Abstract

Ammonia exchange was measured over a mixed suburban forest near a rural area. An average net ammonia flux of $-90\,\mathrm{ng\,m^{-2}\,s^{-1}}$ was measured with corresponding concentration ($[NH_3]$) and deposition velocity of $4.1 \pm 6.5\,\mu\mathrm{g\,m^{-3}}$ and $3.0 \pm 4.6\,\mathrm{cm\,s^{-1}}$, respectively. Subdivision into categories of day/nighttime, wind sector and canopy wetness helped explain fluxes and concentrations. Net fluxes were approximately double for the wind sector exposed to high ammonia levels and during the day. To a certain extent, fluxes (F) followed the maximum flux permitted by turbulent transfer (F_{max}), which was the highest for a dry canopy. When expressed as relative deposition flux (F/F_{maxx}), a wetted canopy seemed to be a more efficient sink than a dry one, especially at nighttime (20–80% increase compared to dry canopy).

Of the net fluxes, 14% represented emission. Emission fluxes occurred mainly during daytime and were important in magnitude for the high $[NH_3]$ wind sector. Emission episodes generally occurred at low ammonia concentrations although high concentrations during dry, warm episodes were also associated with emission events.

The lower deposition efficiency and higher canopy resistance (R_c) at high ammonia levels and at night were indicative of the reduced capacity for leaf surface to retain ammonia, especially when the canopy was dry. It was found that relative humidity (RH) and temperature (T) strongly codetermined the sink strength of the canopy. A warm and humid atmosphere favoured ammonia uptake while conditions with low RH and T impeded rapid canopy uptake, especially at high ammonia levels. Strong interactions between RH and T with the (NH_3/SO_2) molar ratio occurred for certain categories of canopy wetness and day/nighttime. Canopy uptake was further optimized when this ratio was maintained within a certain range.

Keywords: Co-deposition; Emission; Net ammonia flux; Canopy wetness; Canopy resistance; Sulphur dioxide

1. Introduction

Ammonia (NH_3) is a large contributor to nitrogen deposition in European regions exposed to intensive agricultural activities. Ammonia emission originating from point sources such as animal housings or livestock waste storage facilities, and from ground-level area sources such as manure spreading, has enhanced the nitrogen load on semi-natural vegetation in the near- or semi-distant vicinity of such sources (Asman, 1998). In addition to adverse effects of excess nitrogen deposition such as eutrophication and acidification (Hornung and

*Corresponding author. Tel.: +32 54 437119; fax: +32 54 436161.
E-mail address: johan.neirynck@inbo.be (J. Neirynck).

1352-2310/$ - see front matter © 2005 Elsevier Ltd. All rights reserved.
doi:10.1016/j.atmosenv.2005.05.027

Sutton, 1995; Sheppard, 2002), ammonia enhances fine aerosol formation that contributes to turbidity and radiative forcing (Barthelmie and Pryor, 1998; Adams et al., 2001).

Atmospheric turbulence is considered the main rate-determining factor in the exchange of reactive gases between the atmosphere and vegetation. However, several canopy properties act to determine the gradients upon which turbulent transport can mix (Hicks et al., 1987). The canopy sink strength seems to be variable and is driven by physiological processes regulating stomatal conductance and physico-chemical processes influencing uptake at the leaf surface (Flechard et al., 1999). Stomatal ammonia exchange is regulated by the pH-dependent equilibrium between aqueous and gaseous ammonia in the substomatal cavities, determining the direction of the net flux. The compensation point, i.e. the ambient ammonia concentration at which the net flux is zero, is modulated by leaf temperature (Farquhar et al., 1980) but also depends on nitrogen status, plant developmental stage and nitrogen absorptive or assimilative processes (Schjoerring et al., 1998). With regard to deposition to the leaf surface, the role of surface wetness in retaining atmospheric ammonia has already been emphasized (Erisman et al., 1993, 1994; Sutton et al., 1994). In addition, increased attention has been paid to leaf surface water chemistry, particularly interactions of ammonia with other water soluble pollutants such as SO_2 (Cape et al., 1998; Erisman and Wyers, 1993; Fowler et al., 2001). Dynamic simulations of aqueous leaf surface chemistry involving trace gas equilibria, SO_2 oxidation, cation exchange and deliquescent salts on plant surfaces have recently been added to models of ammonia exchange for a moorland site in Scotland (Flechard et al., 1999).

In contrast with fertilized crops, semi-natural vegetation is generally regarded as a perfect sink for atmospheric ammonia (Duyzer et al., 1992; Sutton et al., 1993a). However, several authors (Fowler et al., 1998; Sutton et al., 1993b, 1994; Wyers and Erisman, 1998) reported reduced canopy uptake due to elevated stomatal compensation points as a negative feedback resulting from historical excess nitrogen deposition or volatilization of ammonia from saturated leaf surfaces in dry conditions.

This paper presents ammonia exchange characteristics for a suburban mixed forest near a rural area in Northern Belgium. In a first step, attention has been paid to the role of transport resistances to the net ammonia flux. Fluxes are compared to the maximum flux possible for corresponding rates of turbulent transfer across different categories of canopy wetness, ammonia exposure and stability. Afterwards, the role of canopy resistance (R_c) is discussed. The impact of micrometeorological variables (relative humidity (RH) and temperature (T)) and coexistence of SO_2 on the R_c is examined in order to analyse factors potentially influencing the ammonia uptake capacity of this forest located in a polluted area.

2. Material and methods

2.1. Site characteristics

The forest under investigation is a mixed coniferous/deciduous forest located in the Campine region of Flanders (Belgium, 51°18′N, 4°31′E; Carrara et al., 2003). The forest is relatively small (over 300 ha) and heterogeneous, but of even-height. It is bordered to the North and West by residential areas of the town of Brasschaat at a radius of ca. 500 m from the measurement site. To the South and East the forest extends over 2 km before turning into rural, partially forested terrain. The landscape is a coastal plain, with a gentle (0.3%) slope at a mean elevation of 16 m. The climate is temperate–maritime with a mean annual temperature of 9.8 °C and 770 mm of annual precipitation. Winds are predominately from the SW (>30%).

A self-supporting welded scaffolding was erected to 40 m, with a 9 m^2 ground area and platforms at 9, 15, 18, 23, 31 and 39 m. The tower resides in a 2 ha Scots pine (*Pinus sylvestris* L.) stand of the forest (planting date: 1929) next to a level-II observation plot of the European ICP-Forests network (EC-UN/ECE, 1996) and also figures in the CARBOEUROFLUX research network (http://www.bgc-jena.mpg.de/public/carboeur). The overstory canopy is open, with a tree density of ca. 376 ha^{-1} and a mean height of 21 m. Other Scots pine stands surround (ca. 150–300 m) the measurement tower.

The forest is situated between different pollution climates (Fig. 1). South to westerly winds bring SO_2 and NO_x bearing air masses, coming from either the petrochemical industry in the harbour of Antwerp (15 km to the W), or car emissions on the E19 highway (2 km to the S). Ammonia emission, originating either from cattle stables or manure spreading, originates in rural communities located approximately 10 km North and East with an emission flux density ranging between 4 and 11 ton N km^{-2} yr^{-1}.

2.2. Meteorological and air pollution measurements

Atmospheric measurements were made on the tower. Meteorological data included vertical profiles of air temperature and humidity (psychrometer, Didcot DTS-5A, UK) at 2, 10, 24, 32 and 40 m and wind speed (cup anemometer, Didcot DWR-205G, UK) at 24, 32 and 40 m. At the top of the tower, precipitation (tipping bucket, Didcot DRG-51, UK) was measured. All meteorological sensors were sampled at 0.1 Hz

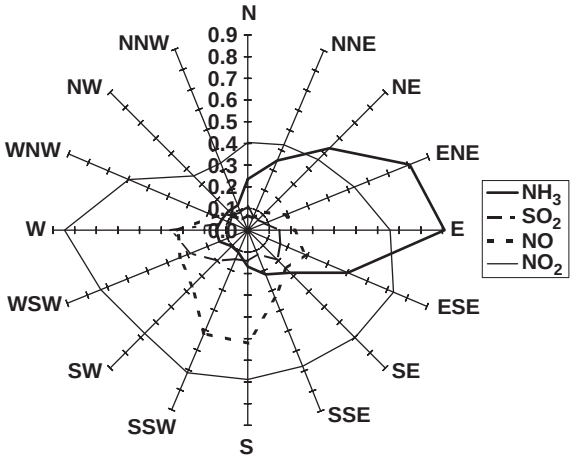

Fig. 1. Mean concentrations of NH_3, NO, NO_2 and SO_2 (in $\mu mol\,m^{-3}$) for 5° wind sectors for the Brasschaat forest site during the measuring period 1999–2001.

and stored as half-hour means on a data logger (Campbell CR10, UK). A sonic anemometer (model SOLENT 1012R2, Gill Instruments, UK) was deployed on a mast above the tower, at 41 m. A leaf wetness sensor (237F, Campbell, UK) was mounted on a boom at 19 m.

An AMANDA continuous wet denuder system (Wyers et al., 1993) was used to measure vertical profiles of NH_3 concentrations at the 23- and 39-m platforms. Continuous-flow denuders collected NH_3 concentrations from pumped ambient air ($28\,l\,min^{-1}$) into a 3.6 mM $NaHSO_4$ absorption solution in the annulus of the rotating denuder. A valve directed the sampled solution (with trapped NH_4^+) from the two denuders towards the waste container or the heated detector (conductivity cell) on the 23 m platform.

Vertical profiles of SO_2 (UV fluorescence, Thermo Instruments, The Netherlands) and NO_x (chemiluminescence, Ecophysics, Switzerland) concentrations included measurements from three inlets above the canopy (24, 32 and 40 m). From each inlet, air was drawn through 53.5 m of tubing at $60\,l\,min^{-1}$ to an instrument shelter, heated to 35 °C, and filtered through a 0.5 mm teflon filter. Each inlet was sampled for 4 min every 15 min, and tubing was flushed before sampling the next inlet.

2.3. Calculation of fluxes and transport resistances

Fluxes (F) were calculated from half-hourly mean values from the Businger–Dyer flux-profile relationships (Dyer and Hicks, 1970; Businger et al., 1971):

$$F = -K\frac{\partial[NH_3]}{\partial z}, \tag{1}$$

where F is the flux (defined positive-upward) and K is the turbulent diffusivity, calculated as:

$$K = \frac{k(z-d)u^*}{\phi}. \tag{2}$$

In this formula k (the von Karman constant) is 0.4, z is the geometric mean of the measurement heights (29.9 m), d is the zero plane displacement ($=19.2$ m) inferred from wind profile measurements, and u^* is the friction velocity determined as the (negative) square root of the kinematic momentum flux measured by eddy covariance. In order to account for stability effects, the universal flux-profile relationships for heat transfer (ϕ_h) were applied (Dyer and Hicks, 1970). Because the concentration measurements were made in the roughness sublayer, turbulent diffusivities estimated by Eq. (2) were corrected by a factor (α) to allow for wake turbulence generated above the canopy (Bosveld, 1991):

$$\phi_h = \begin{cases} L \leqslant 0 \ldots \alpha^* \left(1 - 16\frac{(z-d)}{L}\right)^{-1/2}, \\ L > 0 \ldots \alpha + 5\frac{(z-d)}{L}, \end{cases} \tag{3}$$

where L is the Obukhov length (Monin and Obukhov, 1954). Lacking information on temperature gradients, the factor α was determined empirically from measurements of wind profiles, momentum fluxes and the stability parameter $(z-d)/L$ (analogous to Eq. (3), but for momentum). From near neutral conditions ($-0.02 < (z-d)/L < 0.02$) the correction factor α was determined as 0.87. It should be noted that heat exchange has been found to be more enhanced in the roughness sublayer than momentum (Garratt, 1978).

The deposition velocity (v_d) from the measured flux (F) was obtained by dividing F by the geometric mean of the concentrations $c(=\sqrt{c_{23}c_{39}})$ from the gradient interval z:

$$v_d(z) = \frac{-F}{c(z)} = \frac{1}{R_t} = \frac{1}{R_a + R_b + R_c}. \tag{4}$$

The inverse of v_d defines the total resistance R_t as the sum of resistances associated with aerodynamic (R_a), quasi-laminar boundary layer (R_b) and canopy (R_c) processes. The aerodynamic resistance (R_a) was calculated according to Garland (1978):

$$R_a(z-d) = \frac{1}{ku^*}\left[\ln\left[\frac{z-d}{z_0}\right] - \Psi_h\left(\frac{z-d}{L}\right) + \Psi_h\left(\frac{z_0}{L}\right)\right], \tag{5}$$

where z_0 = roughness length (1.4 m), and $\psi_h((z-d)/L)$ is the integrated stability correction for heat, estimated following Beljaars and Holtslag (1990).

The quasi-laminar resistance R_b is approximated by the formulation presented by Hicks et al. (1987):

$$R_b = \frac{2}{ku^*}\left(\frac{Sc}{Pr}\right)^{2/3}, \quad (6)$$

where Sc and Pr are the Schmidt and Prandtl number, respectively.

R_c was obtained by subtracting R_a and R_b from R_t, after omitting upward fluxes:

$$R_c = \frac{1}{v_d} - R_a - R_b. \quad (7)$$

2.4. Data handling, analysis and statistics

Data were screened to exclude measurement problems and conditions invalidating the use of flux-gradient theory. Friction velocities below $0.1\,m\,s^{-1}$ were rejected because of probable invalid flux-profile relationships. To avoid non-stationarity, data were excluded for which concentrations changes lead to half-hour changes in v_d exceeding $0.01\,m\,s^{-1}$, ($|z/c^*(dc/dt)| < 0.01\,m\,s^{-1}$). Raw sonic anemometer data were submitted to a quality control program in order to reject poor quality data (Vickers and Mahrt, 1997). Gradients were checked for systematic bias between the two heights during episodes of high turbulence ($u^* > 1.5\,m\,s^{-1}$) and strong rain ($>4\,mm\,h^{-1}$) for which gradients were expected to drop to zero. Unequal flow rates due to denuder malfunction or blocked sample lines (presence of soot or pollen) lead to biased gradients, which were omitted from the dataset. In order to reduce the relative errors, concentrations below $0.1\,\mu g\,m^{-3}$ were excluded. Outliers in the data were removed, rejecting any deposition velocity exceeding $2/R_a$.

In order to facilitate interpretation, net flux data were stratified into 16 categories according to day/night conditions, wind sector and canopy wetness. Day was defined as global radiation exceeding $5\,W\,m^{-2}$. The dataset was divided into 5° wind direction sectors, and sectors for which averaged concentrations exceeded $5\,\mu g\,m^{-3}$ were pooled to a high ammonia level wind sector. A further differentiation divided canopy wetness into four classes: rainy conditions (rainfall measured by pluviometer) and non-rainy conditions (no rainfall measured by pluviometer) further subdivided into three classes depending on plate wetness of the leaf wetness sensor: 0% (dry); 0% < 100% (wet); 100% (saturated). Statistical differences among different categories were tested using a Kruskal–Wallis test.

Comparison with F_{max} ($c^*_{max} = c^*(R_a + R_b)^{-1}$) allowed examining the extent to which turbulent transfer drives the ammonia fluxes for the different wind sector and canopy wetness categories. Fluxes were related to F_{max} (continuous variable) and wind sector (factor) using a general linear model:

$$F = \alpha_0 + \alpha_1 W_s + \alpha_2 F_{max} + \alpha_3 W_s F_{max}, \quad (8)$$

where F is the net NH_3 flux, W_s is the wind sector indicator ($W_s = 0$ and $W_s = 1$ for high and low ammonia wind sector, respectively) and α_0, α_1, α_2 and α_3 are fitted parameters.

R_c was further related with T and RH and molar NH_3/SO_2 ratio. The latter was subdivided into three classes differentiating (i) molar ratio < 1: excess of SO_2 over NH_3, (ii) molar ratio between 1 and 5: near-equivalent ratios (close to 2 mol NH_3:1 mol SO_2 to form $(NH_4)_2SO_4$, (iii) molar ratio > 5: excess of ammonia over SO_2.

3. Results

3.1. Flux characteristics

During 23 non-consecutive months (1999–2001), 12,437 half-hourly mean gradients were collected. The low temporal coverage (37%) was caused by instrument failures, interruptions by weekly inter-calibration and frequent maintenance activities. From these gradients only 11,480 could be used for flux calculations because of sonic anemometer failures. After applying the above-mentioned rejection-criteria, 8824 fluxes were retained for detailed analysis from which 54% concerned

Table 1
Average, daytime and nighttime characteristics of ammonia net flux, deposition and emission episodic fluxes

	Total average	Daytime	Nighttime
Net-flux			
n	8824	4734	4090
$[NH_3]$ ($\mu g\,m^{-3}$)	4.1 ± 6.5	4.2 ± 5.4	4.0 ± 7.5
Flux ($\mu g\,m^{-2}\,s^{-1}$)	−0.091 ± 0.176	−0.125 ± 0.222	−0.053 ± 0.085
v_d ($cm\,s^{-1}$)	3.0 ± 4.6	3.5 ± 5.1	2.4 ± 3.9
K ($m^2\,s^{-1}$)	2.7 ± 1.9	3.4 ± 1.8	1.8 ± 1.6
Deposition flux			
n	7588	3912	3675
$[NH_3]$ ($\mu g\,m^{-3}$)	4.4 ± 6.5	4.5 ± 5.2	4.2 ± 7.6
Flux ($\mu g\,m^{-2}\,s^{-1}$)	−0.113 ± 0.174	−0.163 ± 0.216	−0.060 ± 0.086
v_d ($cm\,s^{-1}$)	3.8 ± 4.3	4.7 ± 4.6	2.8 ± 3.8
K ($m^2\,s^{-1}$)	2.6 ± 1.9	3.4 ± 1.8	1.8 ± 1.6
Emission flux			
n	1237	822	415
$[NH_3]$ ($\mu g\,m^{-3}$)	2.7 ± 6.4	3.0 ± 6.3	2.3 ± 6.5
Flux ($\mu g\,m^{-2}\,s^{-1}$)	0.041 ± 0.124	0.055 ± 0.149	0.014 ± 0.026
v_d ($cm\,s^{-1}$)	−2.1 ± 2.7	−2.4 ± 2.7	−1.6 ± 2.4
K ($m^2\,s^{-1}$)	3.2 ± 1.8	3.6 ± 1.7	2.4 ± 1.9

Data include the number of episodes (n), concentration ($[NH_3]$), Flux, deposition velocity (v_d), and eddy diffusivity (K).

daytime conditions (Table 1). An average net ammonia flux of $-0.091\,\mu g\,m^{-2}\,s^{-1}$ was measured over the selected period with corresponding concentration of $4.1\pm6.5\,\mu g\,m^{-3}$ and deposition velocity of $3.0\pm4.6\,cm\,s^{-1}$. Fluxes during daytime ($-0.125\,\mu g\,m^{-2}\,s^{-1}$) were more than two times higher than those at night ($-0.053\,\mu g\,m^{-2}\,s^{-1}$) although ammonia concentrations were not different. The turbulent diffusivity coefficient averaged 3.4 and $1.8\,m^2\,s^{-1}$ for daytime and nighttime conditions, respectively.

To facilitate interpretation, net fluxes were subdivided into deposition and emission episodes. The latter comprised 14% of all net fluxes and were characterized by lower average concentrations ($2.7\,\mu g\,m^{-3}$ vs. $4.4\,\mu g\,m^{-3}$ during deposition). Emission occurred more frequently during daytime (66% of the events) and was four times higher in magnitude than at night.

A further stratification was performed based on wind sector and canopy wetness. Wind directions were subdivided into a western sector (sector 135–360°) with average concentrations of about $2.4\,\mu g\,m^{-3}$ which can be considered as a regional background concentration, and an eastern sector (0–135°) exposed to NH_3-enriched air masses from the intensively managed agricultural areas (Fig. 1). Average concentrations in the eastern sector were of order $10\,\mu g\,m^{-3}$ (Table 2). Net fluxes were approximately double for the high-ammonia wind

Table 2
Average characteristics of net-flux and deposition episodic fluxes, and meteorological conditions for different categories of day/nighttime, wind sector and canopy wetness

	East (high ammonia)				West (low ammonia)				
	Dry	Wet	Saturated	Tot. avg.	Dry	Wet	Saturated	Rainy	Tot. avg.
Daytime									
Net-flux									
n	706	220	235	1203	1623	654	729	339	3531
$[NH_3]$ ($\mu g\,m^{-3}$)	10.7	6.9	5.8	8.8	3.4	2.3	1.6	1.6	2.7
Flux ($\mu g\,m^{-2}\,s^{-1}$)	−0.261	−0.158	−0.110	−0.207	−0.134	−0.089	−0.041	−0.053	−0.097
v_d ($cm\,s^{-1}$)	3.1	3.2	1.8	2.9	4.0	4.1	2.4	5.1	3.7
Deposition flux									
n	616	196	185	1035	1336	536	566	286	2877
$[NH_3]$ ($\mu g\,m^{-3}$)	10.6	7.4	6.6	9.0	3.7	2.5	1.8	1.6	2.9
$[NH_3]$ Gradient ($ng\,m^{-4}$)	96	78	87	89	43	36	23	23	36
Flux ($\mu g\,m^{-2}\,s^{-1}$)	−0.327	−0.189	−0.152	−0.261	−0.173	−0.114	−0.058	−0.068	−0.127
v_d ($cm\,s^{-1}$)	4.0	3.8	3.1	3.8	5.4	5.5	3.9	6.4	5.1
u^* ($m\,s^{-1}$)	0.49	0.43	0.39	0.46	0.59	0.56	0.44	0.63	0.56
R_a+R_b ($s\,m^{-1}$)	23.8	27.9	32.4	26.0	19.6	21.8	29.6	20.8	22.4
K ($m^2\,s^{-1}$)	3.8	3.0	2.5	3.4	3.9	3.2	2.6	3.2	3.4
F_{max} ($\mu g\,m^{-2}\,s^{-1}$)	−0.567	−0.317	−0.279	−0.453	−0.214	−0.136	−0.074	−0.085	−0.160
F/F_{max}	0.76	0.82	0.81	0.78	0.84	0.92	0.81	0.95	0.84
Nighttime									
Net-flux									
n	406	138	288	894	1157	406	1014	423	3196
$[NH_3]$ ($\mu g\,m^{-3}$)	14.7	7.6	8.8	11.0	2.4	2.5	1.8	1.3	2.1
Flux ($\mu g\,m^{-2}\,s^{-1}$)	−0.106	−0.099	−0.111	−0.103	−0.051	−0.039	−0.025	−0.035	−0.038
v_d ($cm\,s^{-1}$)	1.2	1.3	1.9	1.5	2.6	2.2	2.3	4.6	2.6
Deposition flux									
n	380	122	281	840	1003	355	911	378	2835
$[NH_3]$ ($\mu g\,m^{-3}$)	14.9	8.6	8.9	11.3	2.4	2.6	1.8	1.3	2.1
$[NH_3]$ Gradient ($ng\,m^{-4}$)	227	145	200	195	33	40	31	19	31
Flux ($\mu g\,m^{-2}\,s^{-1}$)	−0.114	−0.112	−0.115	−0.111	−0.060	−0.046	−0.030	−0.042	−0.045
v_d ($cm\,s^{-1}$)	1.3	1.8	2.0	1.6	3.2	2.7	2.7	5.5	3.2
u^* ($m\,s^{-1}$)	0.31	0.31	0.25	0.29	0.56	0.43	0.38	0.59	0.48
R_a+R_b ($s\,m^{-1}$)	66.3	54.7	62.2	62.8	31.8	43.5	46.6	24.4	37.6
K ($m^2\,s^{-1}$)	1.0	1.3	0.8	1.0	2.4	1.8	1.5	2.7	2.0
F_{max} ($\mu g\,m^{-2}\,s^{-1}$)	−0.274	−0.205	−0.136	−0.208	−0.108	−0.084	−0.053	−0.064	−0.080
F/F_{max}	0.46	0.60	0.81	0.59	0.55	0.67	0.72	0.85	0.65

sector. As such, they did not clearly reflect the larger differences in ammonia concentrations between these two sectors during day- and nighttime. Consequently, the deposition velocities (v_d), on the contrary, were higher in western sector. The largest differences in deposition velocities between wind sectors were observed during nighttime, which was due to higher (nocturnal) turbulent mixing (higher u^* values) measured in the western sector.

Further differentiation according to canopy wetness yielded subcategories with average net fluxes ranging from -0.030 to $-0.260\,\mu g\,m^{-2}\,s^{-1}$ (Table 2). Dry canopy conditions were predominant (44%), followed by saturated and wet conditions (26% and 16%, respectively). Rainy events constituted 9% of the dataset and were rare for the high ammonia sector. In 5% of the cases, no wetness characteristics were available due to instrument failure. Within each time/sector category, drier canopies were generally associated with substantially higher ammonia concentrations and fluxes (Table 2, Fig. 2). Differences in fluxes among canopy wetness categories were more pronounced during daytime (Table 2, Fig. 2B and C).

3.2. Role of turbulent transfer (R_a+R_b)

When fluxes were compared with F_{max}, the maximum achievable flux allowed by turbulence, it became apparent that turbulent transfer was an important determinant for the magnitude of the fluxes subdivided into day/night, canopy wetness and wind sector classes (Table 2). When hourly averaged net fluxes of ammonia were compared with F_{max}, it was concluded that peaks in fluxes could be largely explained by the shape of the diurnal course of F_{max} (R^2 low ammonia = 0.86; R^2 high ammonia = 0.59). In the high ammonia sector (Fig. 2B), for which net fluxes were substantially altered by large emissions during daytime, a larger agreement with F_{max} was obtained when only deposition episodes were considered (not shown) ($R^2 = 0.78$). The different F_{max} daily patterns between the considered canopy wetness categories (broad, large curve for a dry canopy and lower, smaller peaks for a wet and saturated canopy) reflected differences in concentrations and also in turbulence regime (surface heating).

The highest deposition fluxes were measured during dry, daytime conditions from the high ammonia wind sector (average of $-0.327\,\mu g\,m^{-2}\,s^{-1}$). These elevated values, compared to the fluxes for a non-dry canopy, were mainly due to enhanced turbulent diffusivities since gradient differences were not very pronounced as compared to concentrations (e.g. gradient dry vs. saturated). The average F_{max} for these conditions was $-0.567\,\mu g\,m^{-2}\,s^{-1}$ and resulted from both lower $R_a + R_b$ and higher mean ammonia concentrations. The largest emission fluxes occurred also under similar circumstances. The highest emission fluxes were reached at high ammonia levels during dry, warm episodes (RH < 60% and $T > 15\,^{\circ}C$) (Fig. 3).

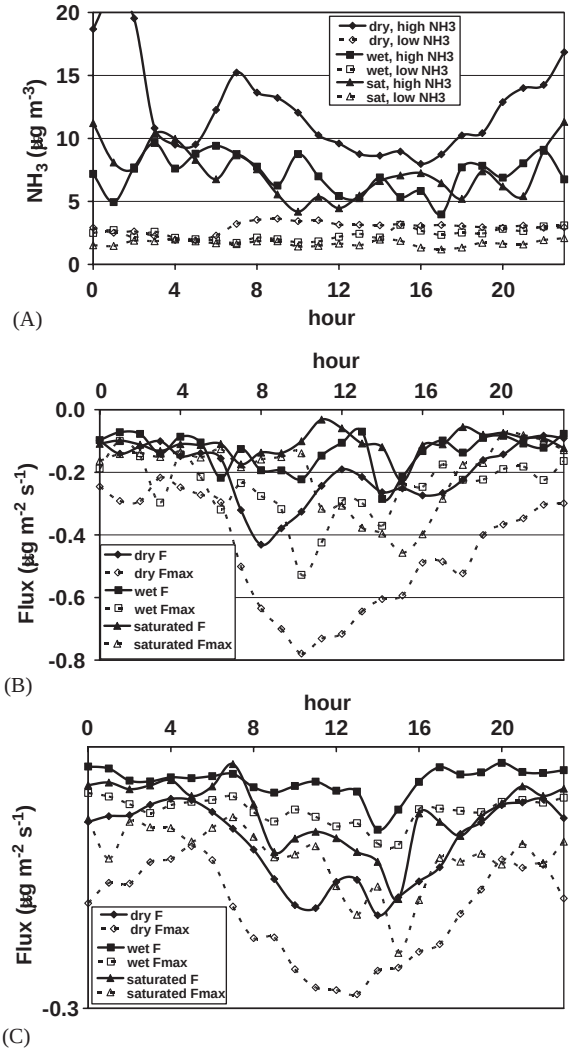

Fig. 2. Mean diurnal course of ammonia concentrations for wind sector exposed to high and low ammonia levels (2A), net-fluxes (F) and maximum fluxes allowed by turbulence (F_{max}) in the wind sector with high (2B) and low ammonia concentrations (2C) for dry, wet and saturated canopy.

Net fluxes from non-rainy events were regressed against sector and maximum achievable flux using a general linear model (Eq. (8), Table 3). Intercepts for the low ammonia sector were significantly higher ($\alpha_1 > 0$) for most categories considered. For all daytime conditions, the slope between ammonia flux and F_{max} was significantly higher for the low ammonia sector ($\alpha_3 > 0$), denoting a more efficient deposition as compared to the high ammonia sector ($\alpha_3 + \alpha_2 > \alpha_2$). With regard to the impact of canopy wetness, the slope between the net

ammonia flux and F_{max} steadily increased from a dry towards a saturated canopy for both the high and low ammonia sector (resp. α_2 and $\alpha_2+\alpha_3$) confirming the shift towards more efficient deposition. The differences in deposition efficiency among sector and canopy wetness could also be observed from the differences in F/F_{maxx} (Table 2). Differences in F/F_{maxx} among canopy wetness were found to be the largest during nighttime (20–80% versus 10% during the day). Nocturnal F/F_{maxx} was found to be, on average, 25% lower compared to daytime F/F_{maxx}.

3.3. Impact of micrometeorological conditions on canopy resistance

Deviations of the flux from F_{max}, especially during nighttime and for a dry canopy indicated substantial resistance to ammonia uptake. R_c for the main categories of wind sector and canopy wetness was substantially higher than zero, even for a non-dry canopy (Table 4). R_cs were twice as high at night compared to daytime and were also higher during exposure to high ammonia levels. The highest median R_c values ($58\,s\,m^{-1}$) were encountered for dry nighttime conditions during high ammonia exposure.

The impact of RH and T on median R_c was examined for the main categories in Table 4. A warm and humid atmosphere (high T and RH) favoured ammonia uptake in non-rainy conditions with daytime R_c values approaching zero. Low RH, on the other hand, was not conducive to canopy uptake, especially at high ammonia concentrations during nighttime. For a dry canopy, medians R_c larger than $100\,s\,m^{-1}$ were reached. A dry atmosphere (low RH) led also to a strong increase in R_c for a saturated canopy during daytime under high ammonia exposure.

Given the impact of ammonia levels on the magnitude of R_c, median R_c values were calculated and plotted against the whole concentration range grouped into percentile classes for corresponding RH/T groups (Fig. 4). Differences in R_c among RH/T groups became more distinct at higher ammonia levels, which could also be observed from Table 4. Although there was a clear tendency for R_c to rise at higher ammonia levels, high R_c values were also measured in the lower range of ammonia concentrations. The strongest raise in R_c to increasing ammonia concentrations was generally observed for cold and dry weather conditions. On the contrary, warm and humid conditions, especially during the day, were favourable to canopy uptake of ammonia; R_c dropped to zero during daytime and responded less to increasing ammonia levels, implying infinite deposition sinks.

The irregular curvature of the R_c-concentration relationships suggested interference with not-accounted variables, as the molar NH_3/SO_2 ratio. Significant influence of the ratio could be found irrespective of canopy wetness but there were strong interactions with the RH and T of the atmosphere (Table 5). During cold and dry weather conditions, an excess of sulphur over ammonia (molar ratios <1) substantially improved the surface uptake for a dry canopy (day- and nighttime). For a saturated canopy, however, this relation was

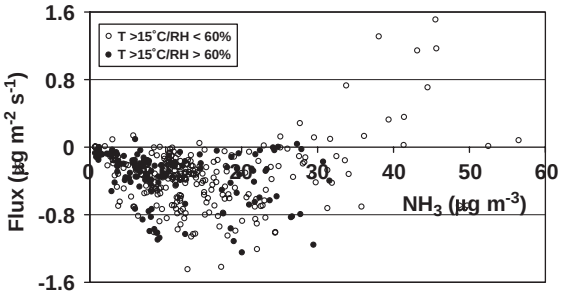

Fig. 3. Dependence of ammonia flux on concentration in the high ammonia wind sector during warm daytime conditions with dry canopy.

Table 3
General linear regressions coefficients of the model (Eq. (8)) relating net NH_3 flux (F) to F_{max} and wind sector, for day- and nighttime and for different wetness conditions

	α_0 ($\mu g\,m^{-2}\,s^{-1}$)	α_1 ($\mu g\,m^{-2}\,s^{-1}$)	α_2 ($\mu g\,m^{-2}\,s^{-1}$)	α_3 ($\mu g\,m^{-2}\,s^{-1}$)	n	R^2
Daytime						
Dry	−0.192***	0.066***	0.618***	0.260***	2320	0.57***
Wet	−0.157***	0.049***	0.782***	0.341***	868	0.54***
Saturated	−0.097***	0.050***	1.097***	0.641***	963	0.54***
Nighttime						
Dry	−0.148***	0.040*	0.583***	0.216**	1557	0.55***
Wet	−0.116***	0.011	0.730***	0.010	539	0.55***
Saturated	−0.106***	0.031***	1.108***	−0.036	1297	0.66***

Levels of statistical significance are *$P<0.05$, **$P<0.01$ and ***$P<0.001$.

Table 4
Impact of relative humidity and temperature on median canopy resistance (R_c) for deposition episodic fluxes across categories of canopy wetness and ammonia exposure (wind sector) during day and nighttime conditions (in $s\,m^{-1}$)

R_c	Dry	Wet	Saturated	Rainy	Total
Daytime					
High ammonia	15 (98)	16 (116)	14 (111)	Na (Na)	15 (102)
Low RH, $T>15\,°C$	14	11	57	Na	
High RH, $T>15\,°C$	7	15	−7	Na	
Low RH, $T<15\,°C$	27	21	78	Na	
High RH, $T<15\,°C$	16	19	8	Na	
Low ammonia	8 (101)	6 (73)	14 (101)	7 (57)	9 (89)
Low RH, $T>15\,°C$	5	9	12	7	
High RH, $T>15\,°C$	3	3	7	9	
Low RH, $T<15\,°C$	15	6	17	3	
High RH, $T<15\,°C$	9	5	20	8	
Nighttime					
High ammonia	58 (249)	29 (124)	20 (83)	Na (Na)	38 (202)
Low RH, $T>11\,°C$	128	42	32	Na	
High RH, $T>11\,°C$	39	19	5	Na	
Low RH, $T<11\,°C$	103	76	19	Na	
High RH, $T<11\,°C$	33	22	24	Na	
Low ammonia	23 (114)	24 (156)	25 (117)	9 (60)	23 (115)
Low RH, $T>11\,°C$	13	17	34	10	
High RH, $T>11\,°C$	15	27	21	24	
Low RH, $T<11\,°C$	35	33	31	4	
High RH, $T<11\,°C$	27	18	18	8	

Average values of R_c are given between brackets for main categories.
Thresholds for RH are based on median values of RH:
daytime: 65%, 77%, 85%, 91% for dry, wet, saturated, rainy conditions, resp.
nighttime: 78%, 85%, 90%, 94% for dry, wet, saturated, rainy conditions, resp.
Median T is 11 °C and 15 °C for night and day, resp.

completely reversed; molar ratios > 1 led instead to lower R_c. The prerequisite of a balanced ratio between the two pollutants (molar ratio 1–5) to enhance the sink strength ($R_c \to 0$) had to be fulfilled for a warm, dry atmosphere during the day and during warm, humid weather conditions at night (dry and wet canopy). The same deposition pattern was also discernible for dry canopy (high RH, high T during the day), wet canopy (high RH, low T during the day) and saturated canopy (low RH, high T at night).

4. Discussion

The results presented here are in accordance with previous reports under similar conditions. Our estimate of the average net flux of ammonia ($-90\,ng\,m^{-2}\,s^{-1}$) agrees with the estimate of $-70\,ng\,m^{-2}\,s^{-1}$ made by Erisman et al. (1996) using the same wet annular denuder sampling system in a similar pollution climate. Likewise, they exceed reported fluxes from other sites with less ammonia loading in Denmark (Andersen et al., 1993), the Midwestern USA (Pryor et al., 2001) and Hungary (Horvath, 2003), where average deposition fluxes were limited to about $-20\,ng\,m^{-2}\,s^{-1}$.

A careful analysis of meteorological and canopy wetness conditions has identified the conditions which correspond to variability in ammonia deposition to this semi-urban forest. Net fluxes were approximately double for the wind sector exposed to high ammonia levels. For a wetted canopy, lower daytime fluxes were observed because of lower turbulent mixing. To a certain extent, fluxes followed the maximum flux permitted by turbulence (F_{max}) which appeared to be the highest when the canopy was dry. When expressed as relative deposition flux (F/F_{maxx}), a wetted canopy seemed to be a more efficient sink than a dry one, in agreement with the observations of Andersen et al. (1999), Duyzer et al. (1992) and Wyers and Erisman (1998). However, even for these optimal conditions, fluxes deviated from F_{max} and a substantial R_c was encountered (Table 4). The highest R_c values were reached in the high ammonia wind sector, which was also reflected in lower deposition velocities and lower F/F_{maxx} compared to the low ammonia sector (Tables 2 and 3). This explains why

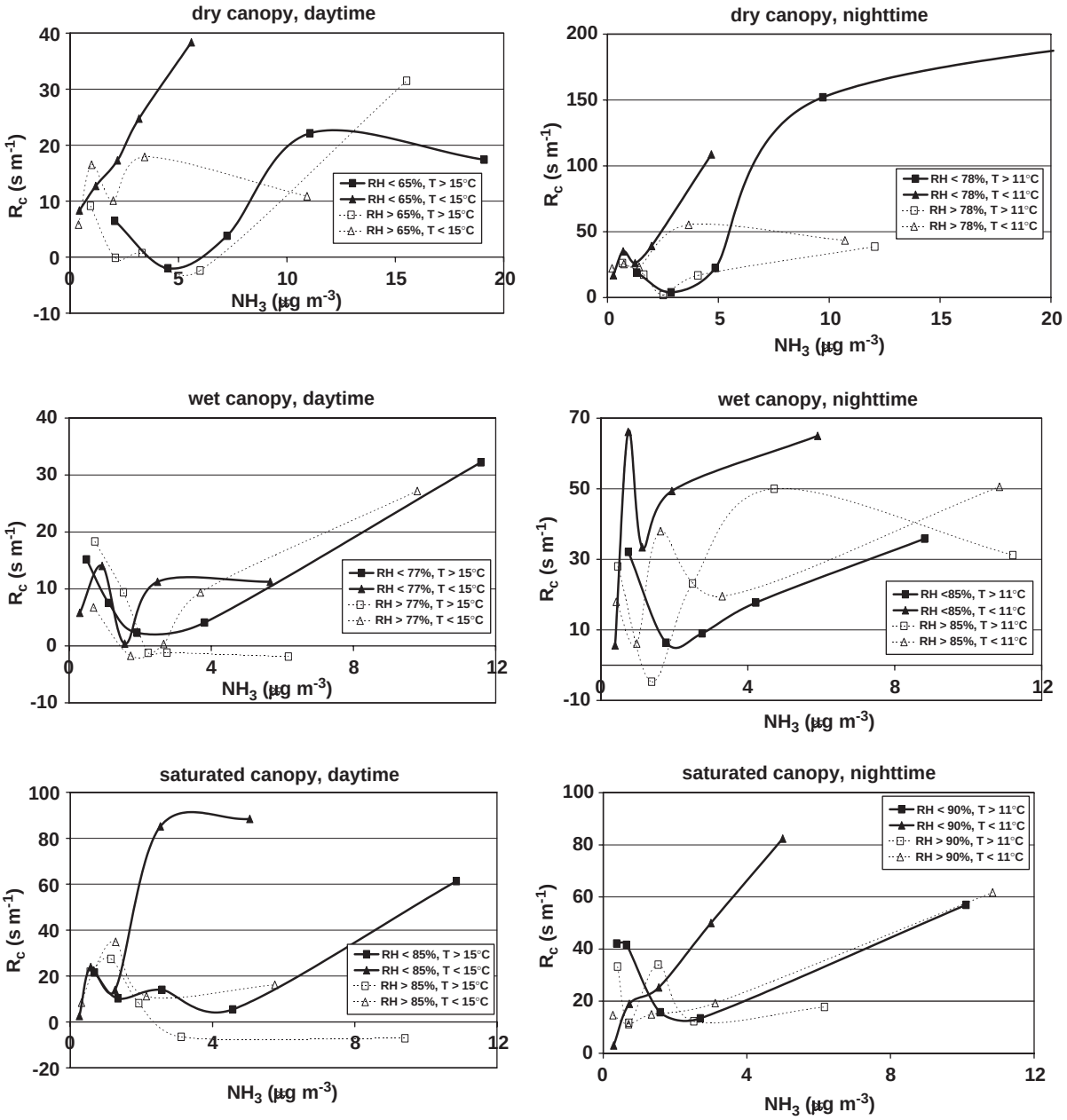

Fig. 4. Relationship between R_c and ammonia concentration classes (based on percentile distribution) for different combinations of relative humidity and temperature during day- and nighttime for dry, wet and saturated canopy.

net fluxes were not as large as might be expected from the difference in ammonia concentration between the two wind sectors.

Emission fluxes represented 14% of the events and mainly occurred during daytime (66% of emission episodes). Emissions episodes occurred mainly in the low ammonia wind sector (82% of emission episodes) but emission fluxes were larger in the sector exposed to high ammonia levels. Reduced ammonia uptake was not only related to the presence of a stomatal compensation point, which might have contributed to emission at low ammonia concentrations during dry events. Emission fluxes were also observed at high ammonia levels during dry episodes ($RH < 60\%$ and $T > 15\,^{\circ}C$) when ammonia saturation of leaf surface could easily be reached. This dual emission pattern is in line with findings of Andersen

Table 5
Dependence of median R_c values (in $s\,m^{-1}$) on different (NH_3/SO_2) ratio ranges across main categories (canopy wetness, day/nighttime) for different combinations of relative humidity and temperature (same groups as defined in Table 4)

	Dry canopy				Wet canopy				Saturated canopy			
	<1	1–5	>5	P	<1	1–5	>5	P	<1	1–5	>5	P
Daytime												
Low RH, $T>15\,^{\circ}C$	5	2	16	0.000	11	5	28	0.000	25	10	34	0.040
High RH, $T>15\,^{\circ}C$	7	−1	18	0.000	9	0	−1	0.015	6	6	−7	0.779
Low RH, $T<15\,^{\circ}C$	13	18	34	0.013	6	8	17	0.791	35	8	10	0.009
High RH, $T<15\,^{\circ}C$	11	13	11	0.493	12	3	20	0.001	17	14	15	0.049
Nighttime												
Low RH, $T>11\,^{\circ}C$	22	22	96	0.000	27	9	33	0.147	37	14	61	0.001
High RH, $T>11\,^{\circ}C$	20	2	41	0.000	28	2	33	0.001	24	14	13	0.153
Low RH, $T<11\,^{\circ}C$	26	92	95	0.000	38	52	44	0.445	34	26	8	0.001
High RH, $T<11\,^{\circ}C$	28	48	33	0.138	17	44	18	0.165	17	14	36	0.055

P levels <0.05 are significant (Kruskal–Wallis test).

et al. (1999) who observed emissions when their Danish site was exposed to ammonia-poor air masses brought by marine winds but also recorded emissions during dry conditions with relatively high ammonia concentrations originating from land winds reflecting evaporation of earlier deposited ammonia from a saturated surface. The impeded leaf surface deposition at high concentrations during dry conditions suggests the presence of micro-scale water layers saturated with ammonia. Changes in meteorological conditions (rise in temperature or decrease in humidity) could readily cause a shift in equilibrium between dissolved NH_x and gaseous ammonia in the leaf boundary layer and trigger emissions from the forest canopy (Andersen et al., 1999; Wyers and Erisman, 1998).

The occurring limitations in ammonia exchange drew our attention to leaf surface chemistry and physical variables controlling R_c. In our study, the impact of RH and T on R_c was demonstrated in relation to ambient ammonia levels. It was found that the canopy constituted almost an infinite sink for ammonia during the day when the atmosphere was humid and warm. Colder and drier weather conditions were unfavourable to ammonia uptake, which rapidly decreased at raised ammonia concentrations. Even for a saturated canopy, an increased R_c was noticed during exposure at high ammonia levels and low RH, suggesting that evaporating water films became less efficient sinks.

The role of RH and T in affecting R_c was also depending on the molar ratio of NH_3/SO_2. Even for a dry canopy the impact of this ratio was decisive, which was somehow surprising since leaf surface deposition would be less likely to occur. Calculated resistances for a dry canopy during the day (median less than $30\,s\,m^{-1}$) were below modelled stomatal resistances (median for dry canopy was about $250\,s\,m^{-1}$). Wyers and Erisman (1998) suggested that at an apparently dry surface, isolated droplets or microscale layers appearing in the stomatal vicinity could still enable ammonia uptake. According to Burkhardt and Eiden (1994), RH in near-stomatal regions can exceed 90% due to transpiration whenever ambient RH is over 50%, enabling deliquescence of hygroscopic particles, which could contribute to the formation of thin water films. According to Fitzgerald (1975), aerosols will be already turned into dissolved droplets at RH ranging from 15% to 80%.

Co-deposition dynamics between ammonia and acid gases such as SO_2 are a matter of much debate (Adema et al., 1986; Flechard et al., 1999; Van Hove et al., 1989). Van Breemen et al. (1982) postulated the hypothesis of mutually enhanced deposition, which was also corroborated by findings of Van Hove et al. (1989). The latter author observed in leaf chamber experiments that stoichiometric adsorption of both gases was strongly enhanced at high vapour pressures in combination with a molar ratio of 4.5. Evidence for stoichiometric-limited adsorption (molar ratio 1–5) occurred at our site mainly during warmer conditions (Table 5). When both gases were near equivalent in concentration, R_c was minimized. There was also a decreased R_c measured for a dry canopy at colder and drier weather conditions when an excess of sulphur over ammonia was prevailing (molar ratio <1). The influence of SO_2 on the R_c of NH_3 via control of the surface pH was also noticed by Erisman and Wyers (1993). Based on gradient measurements of both gases at two Dutch moorlands, they concluded that excess SO_2 compared to NH_3 (acid leaf surface) allowed ammonia to deposit readily with R_c approaching zero. This behaviour, however, was not observed over coniferous forest (Erisman et al., 1994). In some situations, high SO_2 levels over agricultural crops may even deplete NH_3 causing ammonia emission by the

leaves (Sutton et al., 1994). The occurrence of decreased R_c at (NH_3/SO_2) ratios > 5 noticed for a water-saturated canopy (low RH and T) at our site might be, on the other hand, linked to an increased leaf buffer solution. Many authors stressed the role of surface wetness in the deposition dynamics of both gases (Erisman and Wyers, 1993; Sutton et al., 1993b). Larger water pools guaranteed a larger buffer for the alkalinizing effect of ammonia by enhancing CO_2 from the air to dissolve in the liquid phase of the leaf surface (Adema et al., 1986; Flechard et al., 1999; Van Hove et al., 1989). When the canopy is saturated with water, the size of the water pool or the number of water surface layers could increase, ensuring a larger leaf buffer solution consisting of HCO_3/H_2CO_3. The pH-dependent limitations regulating adsorption to a less extended water pool are, under these conditions, probably less important and ammonia can continue to dissolve. In this respect, $(NH_4)HCO_3$ is mentioned as a precursor which can be converted to ammonium bisulphate in a later stage (Van Breemen et al., 1982).

5. Conclusions

Based on this measurement campaign, deposition patterns of ammonia at our nitrogen polluted forest site appear to be very complex. Although flux magnitudes are determined to a large extent by turbulence, there are important canopy interactions that limit ammonia exchange. The predominant role of leaf surface characteristics in changing surface affinities became apparent from the present observations and analysis. The canopy uptake capacity is dependent on (NH_3/SO_2) molar-ratio-dependent interactions with RH and T. This confirms the important role of leaf surface deposition in ammonia exchange, either dominating or occurring in parallel with stomatal pathways.

Future research should thus focus not only on calculations of the stomatal compensation point, but also on the degree of ammonia saturation on leaf surfaces. Estimating the possible extent of deposition and simulating the bidirectional flux of ammonia will require a better estimate of canopy water storage, calculations of the amount of ammonia accumulated in previous events and information about leaf surface composition or acidity (via previous acid pollutant fluxes). Finally, the inclusion of memory effects will require the availability of complete records, which were not available in the present study.

Acknowledgements

The purchase of the AMANDA monitor and the employment of our gratefully acknowledged expert Yves Buidin were possible thanks to the financial framework of the VLINA (Flemish Impulse Program on Nature Development). We thank Dr. J.W. Erisman for his useful advice. This project was performed under the authority of the Flemish minister of the Environment. ASK is a *Ramon y Cajal* fellow, supported by the Spanish Ministry of Science and Technology, National Scientific Research Plan for Technological Development and Innovation.

References

Adams, P.J., Seinfeld, J.H., Koch, D., Mickley, L., Jacob, D., 2001. General circulation model assessment of direct radiative forcing by the sulfate–nitrate–ammonium–water inorganic aerosol system. Journal of Geophysical Research 106, 1097–1111.

Adema, E.H., Heeres, P., Hulskotte, J., 1986. On the dry deposition of NH_3, SO_2, and NO_2 on wet surfaces in a small scale wind tunnel. In: Hartman, H.F. (Ed.), Proceedings of the Seventh World Clean Air Congress, vol. 2. Clean Air Society of Australia and New Zealand, pp. 1–8.

Andersen, H.V., Hovmand, M., HummelshØj, P., Jensen, N.O., 1993. Measurements of ammonia flux to a spruce stand in Denmark. Atmospheric Environment 27A, 189–202.

Andersen, H.V., Hovmand, M., HummelshØj, P., Jensen, N.O., 1999. Measurements of ammonia concentrations, fluxes and dry deposition velocities to a spruce forest 1991–1995. Atmospheric Environment 33, 1367–1383.

Asman, W.A.H., 1998. Factors influencing local dry deposition of gases with special reference to ammonia. Atmospheric Environment 32, 415–421.

Barthelmie, R.J., Pryor, S.C., 1998. Implications of ammonia emissions for fine aerosol formation and visibility impairment—a case study from the lower Fraser Valley, British Columbia. Atmospheric Environment 32, 345–352.

Beljaars, A.C.L., Holtslag, A.A.M., 1990. Description of a software library for the calculation of surface fluxes. Environmental Software 5, 60–68.

Bosveld, F.C., 1991. Turbulent Exchange Coefficients over a Douglas Fir Forest. Final report Dutch Priority Programme on Acidification, Project 190.1. Royal Netherlands Meteorological Institute (KNMI), De Bilt.

Burkhardt, J., Eiden, R., 1994. Thin water films on coniferous needles. Atmospheric Environment 28, 2001–2017.

Businger, J.A., Wyngaard, J.C., Izumi, Y., Bradley, E.F., 1971. Flux-profile relationships in the atmospheric surface layer. Journal of Atmospheric Science 28, 181–189.

Cape, J.N., Sheppard, L.J., Binnie, J., Dickinson, A.L., 1998. Enhancement of the dry deposition of sulphur dioxide to a forest in the presence of ammonia. Atmospheric Environment 32, 519–524.

Carrara, A., Kowalski, A.S., Neirynck, J., Janssens, I.A., Curiel Yuste, J., Ceulemans, R., 2003. Net ecosystem CO_2 exchange of mixed forest in Belgium over 5 years. Agricultural and Forest Meteorology 119, 209–227.

Duyzer, J.H., Verhagen, H.L.M., Westrate, J.H., Bosveld, F.C., 1992. Measurement of the dry deposition flux of NH_3 onto coniferous forest. Environmental Pollution 75, 3–13.

Dyer, A.J., Hicks, B.B., 1970. Flux-gradient relationships in the constant flux layer. Quarterly Journal of the Royal Meteorological Society 96, 715–721.

Erisman, J.W., Wyers, G.P., 1993. Continuous measurements of surface exchange SO_2 and NH_3; implications for their possible interaction in the deposition process. Atmospheric Environment 27A, 1937–1949.

Erisman, J.W., Vanelzakker, B.G., Mennen, M.G., Högenkamp, H., Zwart, E., Van den Beld, L., Römer, F.G., Bobbink, R., Heil, G., Raessen, M., Duyzer, J.H., Verhage, H., Wyers, G.P., Otjes, R.P., Möls, J.J., 1994. The Elspeetsche Veld experiment on surface exchange of trace gases: summary of results. Atmospheric Environment 28, 487–496.

Erisman, J.W., Mennen, M., Hogenkamp, J., Kemkers, E., Godhart, D., van Pul, A., Draaijers, G., Duyzer, J., Wyers, P., 1994. Dry deposition monitoring of SO_2, NH_3 and NO_2 over a coniferous forest. In: Borrell, P.M., Borrell, P., Cvitas, T., Seiler, W. (Eds.), The Proceedings of EUROTRAC Symposium '94. The Hague, The Netherlands, pp. 655–659.

Erisman, J.W., Draaijers, G.P.J., Mennen, M.G., Hogenkamp, J.E.M., van Putten, E., Uiterwijk, W., Kemkers, E., Wiese, H., Duyzer, J.H., Otjes, R., Wyers, G.P., 1996. Towards development of a deposition monitoring network for air pollution of Europe. Deposition monitoring over the Speulder forest; Report no. 722108014. RIVM, Bilthoven, The Netherlands, p. 80.

Farquhar, G.D., Firth, P.M., Wetselaar, R., Weir, B., 1980. On the gaseous exchange of ammonia between leaves and the environment: determination of the ammonia compensation point. Plant Physiology 66, 710–714.

Fitzgerald, J.W., 1975. Approximation formulas for the equilibrium size of an aerosol particle as a function of its dry size and composition and the ambient relative humidity. Journal of Applied Meteorology, 1044–1049.

Flechard, C.R., Fowler, D., Sutton, M.A., Cape, J.N., 1999. A dynamic chemical model of bi-directional ammonia exchange between semi-natural vegetation and the atmosphere. Quarterly Journal of the Royal Meteorological Society 125, 2611–2641.

Fowler, D., Flechard, D., Sutton, M.A., Storeton-West, R., 1998. Long term measurements of the land-atmosphere exchange of ammonia over moorland. Atmospheric Environment 32, 453–459.

Fowler, D., Sutton, M.A., Flechard, C., Cape, J.N., Storeton-West, Coyle, M., Smith, R.I., 2001. The control of SO_2 dry deposition on to natural surfaces by NH_3 and its effects on regional deposition. Water, Air, and Soil Pollution: Focus 1, 39–48.

Garland, J.A., 1978. Dry and wet removal of sulfur from the atmosphere. Atmospheric Environment 12, 349–362.

Garratt, J.R., 1978. Flux profile relations above tall vegetation. Quarterly Journal of the Royal Meteorological Society 104, 199–211.

Hicks, B.B., Baldocchi, D.D., Meyers, T.P., Hosker, R.P., Matt, D.R., 1987. A preliminary multiple resistance routine for deriving dry deposition velocities from measured quantities. Water, Air, and Soil Pollution 36, 311–330.

Hornung, M., Sutton, M.A., 1995. Impacts of nitrogen deposition in terrestrial ecosystems. Atmospheric Environment 29, 3395–3396.

Horvath, L., 2003. Dry deposition velocity of PM2.5 ammonium sulfate particles to a Norway spruce forest on the basis of S- and N-balance estimations. Atmospheric Environment 37, 4419–4424.

Monin, A.S., Obukhov, A.M., 1954. Basic laws of turbulence mixing in the ground layer of the atmosphere. Trudii Geo Phisical Institut, Academy Nauk SSSR 151, 163–187.

Pryor, S.C., Barthelmie, R.J., Sørensen, L.L., Jensen, B., 2001. Ammonia concentrations and fluxes over a forest in the midwestern USA. Atmospheric Environment 35, 5645–5656.

Schjoerring, J.K., Husted, S., Mattsson, M., 1998. Physiological parameters controlling plant-atmosphere ammonia exchange. Atmospheric Environment 32, 491–498.

Sheppard, S.C., 2002. Three approaches to define the ecotoxicity threshold for atmospheric ammonia. Canadian Journal of Soil Science 82, 341–354.

Sutton, M.A., Fowler, D., Moncrieff, J.B., 1993a. The exchange of atmospheric ammonia with vegetated surfaces. I: Unfertilized vegetation. Quarterly Journal of the Royal Meteorological Society 119, 1023–1045.

Sutton, M.A., Pitcairn, C.E.R., Fowler, D., 1993b. The exchange of ammonia between the atmosphere and plant communities. Advances in Ecological Research 24, 301–393.

Sutton, M.A., Asman, W.A.H., SchjØrring, J.K., 1994. Dry deposition of reduced nitrogen. Tellus 46, 255–273.

Vickers, D., Mahrt, L., 1997. Quality control and flux sampling problems for tower and aircraft data. Journal of Atmospheric and Oceanic Technology 14, 512–526.

Van Breemen, N., Burrough, P.A., Velthorst, E.J., Dobben, H.F., van Wit, T., de Ridder, T.B., Reinders, H.F.R., 1982. Soil acidification from atmospheric ammonium sulphate in forest canopy throughfall. Nature 299, 548–550.

Van Hove, L.W.A., Adema, E.H., Vredenberg, W.H., Pieters, G.A., 1989. A study of the adsorption of NH_3, and SO_2 on leaf surfaces. Atmospheric Environment 23, 1479–1486.

Wyers, G.P., Erisman, J.W., 1998. Ammonia exchange over coniferous forest. Atmospheric Environment 32, 441–451.

Wyers, G.P., Otjes, R.P., Slanina, J., 1993. A continuous-flow denuder for the measurement of ambient concentrations and surface-exchange fluxes of ammonia. Atmospheric Environment 27A, 2085–2090.